

# Packaging Using Microelectromechanical Technologies and Planar Components

Kazuaki Takahashi, *Member, IEEE*, Ushio Sangawa, Suguru Fujita, Michiaki Matsuo, Takeharu Urabe, Hiroshi Ogura, and Hiroyuki Yabuki

**Abstract**—A novel millimeter-wave packaging structure was developed in which a micromachined low-loss planar component and flip-chip devices were integrated on a silicon substrate. A low-loss planar filter was achieved on a 7-mm-square silicon substrate employing an inverted microstrip line and a unique resonator. High attenuation in the stopband was also obtained by introducing a pole control technique. Fabrication of a compact *K*-band receiver front-end incorporating a built-in filter was realized using multilayered benzocyclobutene (BCB) and flip-chip bonding techniques. Furthermore, we propose an alternative BCB suspended structure and demonstrate a planar antenna for *Ka*-band applications. These technologies bring to reality high-performance compact packaged systems in millimeter-wave region applications.

**Index Terms**—BCB, flip-chip, inverted microstrip, micromachining, silicon, suspended line.

## I. INTRODUCTION

RECENTLY, the demand for broad-band microwave and millimeter-wave communication systems has been rapidly increasing. Low-loss passive components are required in a planar structure and, as such, a number of micromachined structures employing anisotropic etching have been proposed [1], [2]. The current hurdle is how to combine active and passive devices into a single package. New proposals for flip-chip bonding on a silicon substrate incorporating dielectric multilayer thin films have been reported [3]–[5]. However, problems still remain in the fabrication of low-loss planar components on silicon for completely integrated compact packaged systems. In order to realize built-in low-loss components, we successfully developed a *K*-band filter [6] and antenna [7] employing a quartz substrate. This paper describes a new packaging structure on a micromachined silicon substrate containing low-loss planar components (proposed in Section II). Adoption of an inverted microstrip line (IMSL) using silicon deep trench etching enabled us to realize a built-in low-loss filter on silicon. In Section III, the inverted microstrip-line characteristics are discussed in detail and a planar filter on the inverted structure is demonstrated. Low-loss characteristics were achieved employing a dual-mode ring (DMR) resonator [9], [10] fabricated completely from silicon. In addition, pole

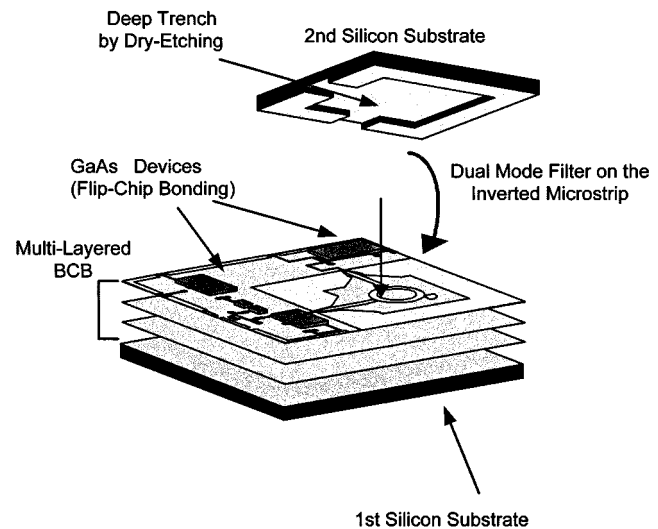


Fig. 1. Cross-sectional view of the proposed packaging structure for millimeter-wave radio systems using micromachining technology.

frequency-control methodology for the dual-mode resonator realized high attenuation in the target frequency. In Section IV, a *K*-band receiver front-end hybrid integrated circuit (HIC) demonstrates the application of multilayered benzocyclobutene (BCB) and flip-chip bonding techniques in the developed filter. Furthermore, we propose a micromachined BCB membrane structure as an alternative packaging structure for *Ka*-band applications in Section V. A *Ka*-band circular polarized patch antenna on the membrane structure was successfully developed.

## II. THREE-DIMENSIONAL MILLIMETER-WAVE PACKAGING STRUCTURE USING SILICON MICROMACHINING

Fig. 1 shows a cross-sectional view of the proposed three-dimensional millimeter-wave integrated-circuit (IC) structure. Multilayered BCB was formed on the first silicon substrate. Passive elements, such as filters and matching circuits that can be formed into each layer, and active devices were assembled on the top layer using flip-chip bonding technology. In the filter section, micromachined silicon (second silicon) with a ground metal-filled shallow cavity was used to cover the filter pattern. The illustrated packaging structure is basically a three-dimensional HIC using silicon as a base substrate. The application of silicon as opposed to the common application of GaAs enables the cost of the substrate as a whole to be reduced. In addition, the filter is formed on the silicon monolithically, reducing the interconnection loss between the filter and its surrounding circuits. However, silicon is not a loss-free material, though low-loss

Manuscript received February 26, 2001. This work was supported by the Telecommunications Advancement Organization of Japan.

K. Takahashi, U. Sangawa, S. Fujita, M. Matsuo, and H. Yabuki are with the Mobile Communication Research Laboratory, Matsushita Research Institute Tokyo Inc., Kawasaki 214-8501, Japan.

T. Urabe and H. Ogura are with the Advanced Technology Research Laboratories, Matsushita Electric Industrial Company Ltd., Kawasaki 214-8501, Japan.

Publisher Item Identifier S 0018-9480(01)09386-3.

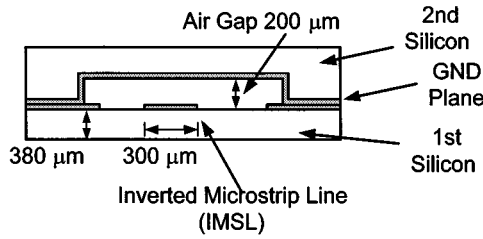


Fig. 2. Cross-sectional view of the proposed IMSL on silicon.

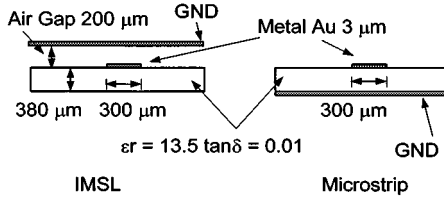
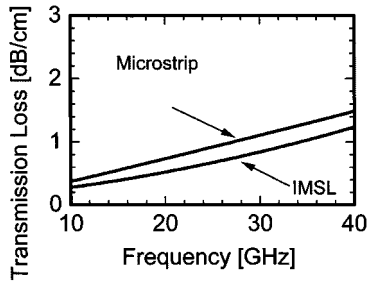


Fig. 3. Calculated results of the IMSL transmission loss compared to a conventional MSL using the same silicon substrate.

characteristics are essential for the filter. In reducing the loss found with silicon, an inverted structure can be considered since air is an ideal loss-free material.

### III. SILICON MICROMACHINED PLANAR COMPONENTS

#### A. IMSL Structure

Fig. 2 shows the cross-sectional view of the proposed transmission line using silicon micromachining. The transmission line consists of two silicon substrates: a silicon substrate (first silicon) on which the transmission line is patterned, and a micromachined silicon substrate (second silicon) with a shallow metal-covered cavity. The two substrates are bonded together to produce the IMSL structure. The IMSL structure utilizes the air gap formed between the line and cavity to obtain a low transmission loss owing to the application of air.

Fig. 3 compares the calculated transmission loss of the IMSL against a conventional microstrip line (MSL) in a 380-μm-thick silicon substrate. A commercial electromagnetic (EM) simulator-based (*em*, Sonnet Software, Liverpool, NY) method of moments (MoM) was applied in this calculation. Calculations were obtained from the following to exclude the influence of the return loss:

$$\text{LOSS} = \left| 10 \cdot \log (|S_{11}|^2 + |S_{21}|^2) \right| \text{ dB.} \quad (1)$$

Both transmission lines were formed on the same dielectric substrate, and the cavity depth for the IMSL was fixed at 200 μm, as described below. The results show that the trans-

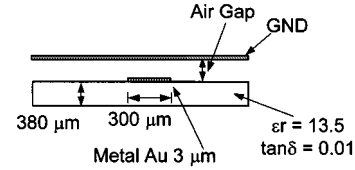
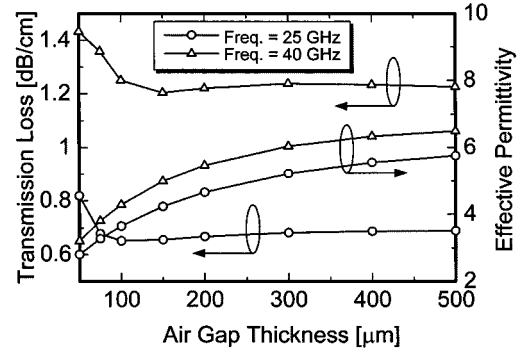


Fig. 4. Calculated IMSL transmission loss with variation in air-gap thickness.

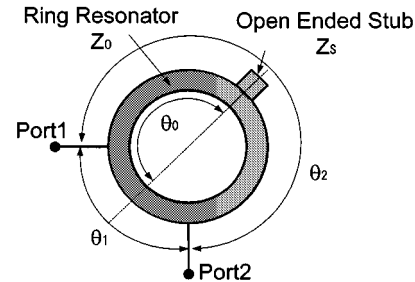


Fig. 5. Circuit schematic of a DMR filter.

mission loss can be reduced for the IMSL in comparison with conventional MSL lines. This is because a portion of the EM field propagates through the air gap. A calculated transmission loss of 0.6 dB/cm at 25 GHz was obtained for the IMSL.

Fig. 4 shows the calculated results for varying air-gap thickness. The transmission loss increased significantly when the air gap was less than 100 μm, though the effective permittivity was low. The reason for this is that conductor loss increases significantly since the EM field is concentrated on the edge of the line. Selection of the optimum air gap then becomes a factor of RF characteristics and productivity. A 200-μm air gap was selected for the following planar components.

#### B. DMR Filter

The above results clearly indicated that low-loss characteristics could be obtained, leading us to our next goal of realizing a low-loss circuit configuration within the filter itself. Thus, a DMR filter, as shown in Fig. 5, was newly adopted. The most useful feature of the DMR filter is the inherently low radiation loss, an important factor in simplifying shield structure complexity, since there are no open ends in the ring shape. Another feature is the inclusion of two attenuation poles on the upper and lower sides of the passband where high attenuation in the stop-band can be easily obtained in a few stages. In order to couple between the two orthogonal resonance modes in the ring resonator, a point of perturbation should be located on the resonator

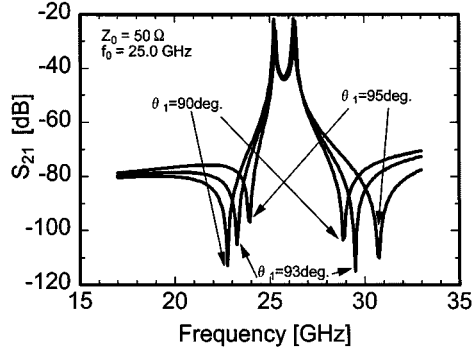


Fig. 6. Frequency shift of the attenuation poles from varying the electrical length of  $\theta_1$ .

symmetrically between the input and output ports. The attenuation poles are expected to appear under the following conditions:

$$\theta_2 - \theta_1 \cong 180^\circ \quad (2)$$

where  $\theta_1$  and  $\theta_2$  are the electrical lengths between both ports ( $\theta_1 < \theta_2$ ). When  $\theta_1 = 90^\circ$ , the attenuation pole frequency  $f_{\text{pole}}$  can be derived from the following equation [10]:

$$\begin{aligned} \sin\left(\frac{\pi}{2}f'_p\right) + \sin\left(\frac{3}{2}\theta_0 f'_p\right) - \frac{1}{K_Z} \sin^2\left(\frac{3}{4}\theta_0 f'_p\right) \tan\left(\frac{3}{4}\theta_0 f'_p\right) \\ = 0 \\ f'_p = \frac{f_{\text{pole}}}{f_0} \\ K_Z = \frac{Z_S}{Z_0} \end{aligned} \quad (3)$$

where  $f_0$  is the resonant frequency of the ring resonator,  $\theta_0$  is the half electrical length of the ring resonator,  $Z_0$  is the characteristic impedance of the ring resonator,  $Z_S$  is the characteristic impedance of the open-ended stub where  $K_Z$  is the impedance ratio between the MSL of the resonator and the open-ended stub. The relation in (2) implies that the pole frequency will rise in accordance to an enlarged  $\theta_1$ , due to a decrease in electrical length between the two different paths of both ports ( $\theta_2 - \theta_1$ ). To confirm this assumption, the pole frequencies were calculated with  $\theta_1$  as a parameter using a general-purpose circuit simulator with coupling to both ports. The calculated pole frequencies are shown in Fig. 6. The results proved that the pole frequency was shifted upward by enlarging  $\theta_1$  without fluctuation in passband frequency. Here, we intentionally designed the pole frequency by adjusting  $\theta_1$ , to suppress the local-oscillator (LO) signal located 1.72 GHz below the RF signal (25.0 GHz). A photograph of the developed filter and experimental results are shown in Figs. 7 and 8, respectively. The chip size was 7 mm  $\times$  7 mm, center frequency designed at 25.0 GHz, passband width was over 500 MHz, and the insertion loss of the passband was less than 1.0 dB. Calculated unloaded  $-Q(Q_U)$  from the filter response rose above 230.

#### IV. RECEIVER FRONT-END IC WITH MICROMACHINED FILTER

Applying the above-mentioned technologies, we designed and fabricated a  $K$ -band front-end IC incorporating a micromachined RF filter. Fig. 9 shows a block diagram of the receiver

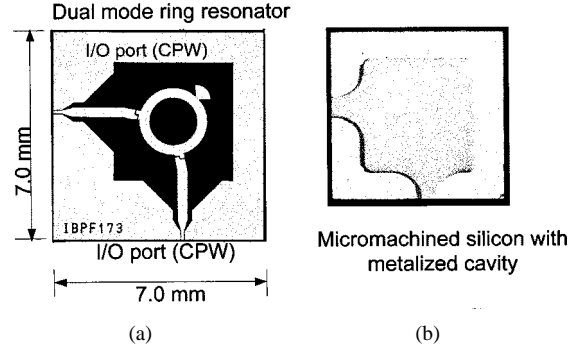


Fig. 7. Fabricated dual-mode filter using silicon substrate. (a) Filter pattern. (b) Micromachined cavity as ground plane.

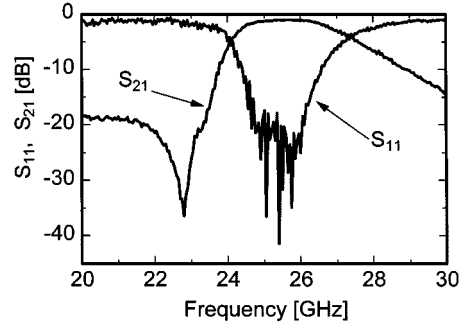


Fig. 8. Measured frequency response of the fabricated 25-GHz micromachined filter.

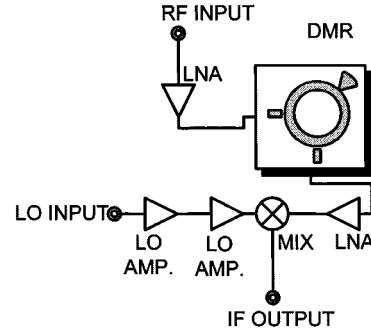


Fig. 9. Block diagram of the 25-GHz receiver front-end IC incorporating a micromachined filter.

front-end IC. Microwave and monolithic millimeter-wave integrated circuits (MMICs) were employed for the amplifiers (low-noise amplifiers and a local amplifier) and a discrete pseudomorphic high electron-mobility transistor (p-HEMT) was applied for the down converter, respectively. All components were incorporated into an overall chip size of 11  $\times$  11 mm<sup>2</sup>, as shown in Fig. 10. A maximum overall conversion gain of 26 dB was obtained, while noise figure was less than 4 dB. These results showed minimal degradation from their expected performance. Frequency characteristics are shown in Fig. 11. The measured overall conversion gain agrees well with that calculated from the characteristics of each individual unit. Though a ripple of about 2 dB or more was observed in the desired band (25.0 GHz  $\pm$  250 MHz), the DMR filter displayed sufficient suppression at its designed stopband, i.e., a suppression of above 28 dB at 22.8 GHz. The ripple near the passband

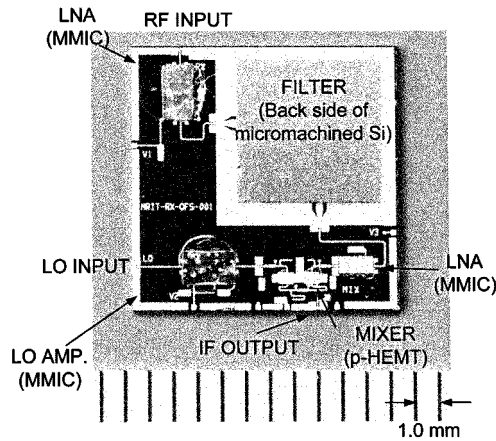


Fig. 10. Fabricated 25-GHz receiver front-end IC incorporating a micromachined filter.

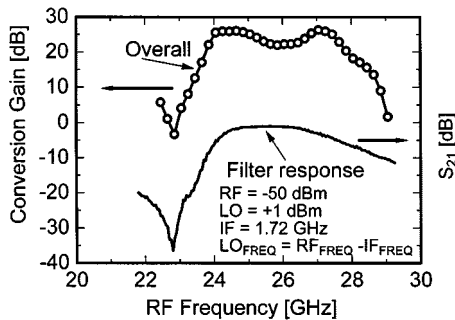


Fig. 11. Measured frequency characteristics of the receiver front-end in comparison with filter response itself.

was caused by the down-converter characteristics itself since the drain LO injection mixer has narrow-band characteristics.

## V. BCB SUSPENDED STRUCTURE FOR ALTERNATIVE PACKAGING STRUCTURE

### A. BCB Suspended Structure

Additional low-loss characteristics are required in higher frequency-band applications, such as *Ka*- or *V*-bands. Fig. 12 shows an alternative packaging layout for a millimeter-wave IC incorporating a BCB membrane structure. The membrane structure is very effective in eliminating the effect of the silicon. Additional bottom trench etching of the base silicon substrate (first silicon) can easily achieve such a structure. The planar components were suspended on a 20- $\mu\text{m}$  BCB membrane. This structure allows high-performance planar components to be formed on the silicon monolithically even in *Ka*- or *V*-bands. As shown in Fig. 13, a transmission loss of 0.3 dB was calculated for a 1-cm length of the BCB suspended structure with a 200- $\mu\text{m}$  air gap at 40 GHz. The transmission loss was reduced to one-quarter or less for an IMSL on a 380- $\mu\text{m}$  silicon configuration with a 200- $\mu\text{m}$  air gap.

### B. Planar Components

As one of the applications of the suspended structure, a *Ka*-band patch antenna was developed. Low-loss characteristics of the suspended line can be expected realizing a high-efficiency antenna. Patch antennas are the most simple

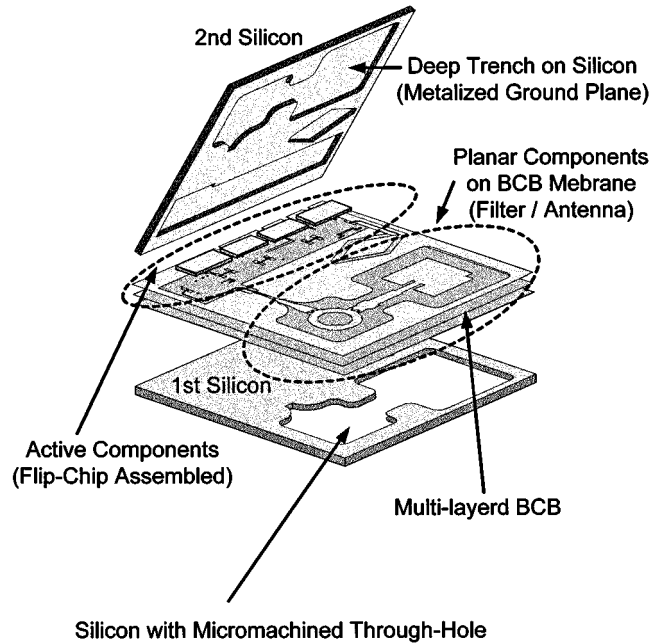


Fig. 12. Alternative packaging structure using a micromachined BCB membrane structure.

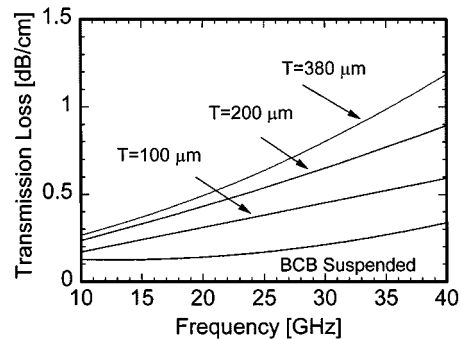
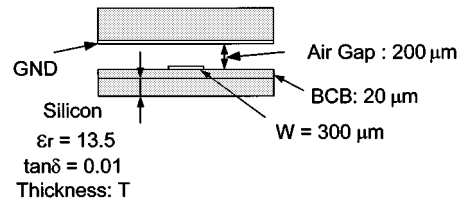


Fig. 13. Calculated transmission loss as a parameter of silicon thickness (0  $\mu\text{m}$  of thickness (T) means that the BCB is suspended).

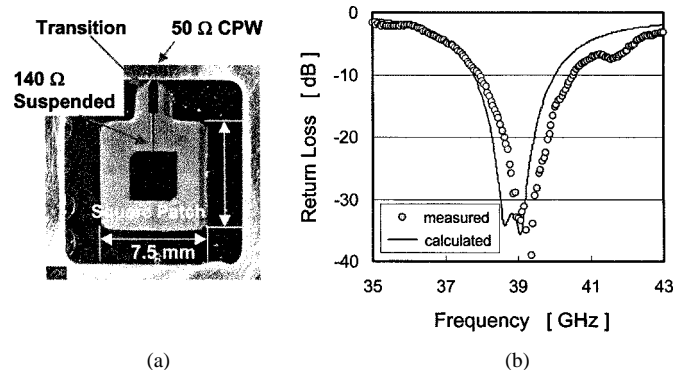


Fig. 14. Fabricated *Ka*-band patch antenna using a micromachined BCB suspended structure. (a) Photograph. (b) Impedance characteristics.

and easy to design. We designed a circular polarized patch antenna with a single radiation element containing two orthogonal resonance modes, as shown in Fig. 14(a). Broad-band characteristics can be achieved by applying a BCB suspended structure to the resonator-type antenna because the permittivity is close to that of air. The developed patch antenna achieved a bandwidth of 6.7%, as shown in Fig. 14(b).

## VI. CONCLUSIONS

We have proposed a new packaging structure adopting silicon micromachining for millimeter-wave radio communications. A micromachined IMSL enabled us to realize low-loss planar components on silicon in millimeter-wave bands. A high-performance  $K$ -band filter was realized on compact silicon,  $7\text{ mm} \times 7\text{ mm}$ , employing unique DMR and pole frequency methodologies. A fabricated  $K$ -band receiver front-end IC incorporating the micromachined filter proved that high productivity and high performance were possible with the proposed structure. Furthermore, a BCB membrane structure was also proposed and described. A  $Ka$ -band antenna was developed as an application example, and good characteristics were demonstrated. Micromachined packaging structures are very effective in realizing and producing multifunctional system in a package even in the millimeter-wave region.

## ACKNOWLEDGMENT

The authors gratefully acknowledge Dr. M. Makimoto, Matsushita Research Institute Tokyo Inc., Kawasaki, Japan, Dr. M. Sagawa, Matsushita Research Institute Tokyo Inc., Kawasaki, Japan, and K. Nagao, Matsushita Communication Industrial Company Ltd., Yokohama, Japan, for their encouragement and helpful suggestions.

## REFERENCES

- [1] R. F. Drayton and L. P. B. Katehi, "Development of self-packaged high frequency circuits using micromachining techniques," *IEEE Trans. Microwave Theory Tech.*, vol. 43, pp. 2073–2080, Sept. 1995.
- [2] S. V. Robertson, L. P. B. Katehi, and G. M. Rebeiz, "Micromachined self-packaged  $W$ -band bandpass filters," in *IEEE MTT-S Int. Microwave Symp. Dig.*, 1995, pp. 1543–1546.
- [3] K. Takahashi, T. Yoshida, H. Sakai, and M. Sagawa, "An advanced millimeter-wave flip-chip IC integrating different kinds of active devices," in *IEEE MTT-S Int. Microwave Symp. Dig.*, 1996, pp. 1919–1922.
- [4] K. Takahashi, S. Fujita, H. Yabuki, T. Yoshida, Y. Ikeda, H. Sakai, and M. Sagawa, "Development of  $K$ -band front-end devices for broadband wireless communication systems using millimeter-wave flip-chip IC technology," *IEICE Trans. Electron.*, vol. E81-C, no. 6, pp. 827–833, 1998.
- [5] K. Takahashi, H. Ogura, and M. Sagawa, "Miniaturized millimeter-wave hybrid IC technology using non-photosensitive multi-layered BCB thin films and stud bump bonding," *IEICE Trans. Electron.*, vol. E82-C, no. 11, pp. 2029–2037, 1999.
- [6] U. Sangawa, S. Fujita, K. Takahashi, A. Ono, H. Ogura, and H. Yabuki, "Micromachined millimeter-wave devices with three dimensional structure," in *Asia-Pacific Microwave Conf. Dig.*, 1998, pp. 505–509.
- [7] S. Fujita, U. Sangawa, K. Takahashi, K. Goho, S. Takeyama, H. Ogura, and H. Yabuki, "Millimeter-wave transceiver MCM using multi-layer BCB with integrated planar antenna," in *Proc. 29th European Microwave Conf.*, vol. 2, 1999, pp. 91–93.
- [8] K. Takahashi, S. Fujita, U. Sangawa, A. Ono, T. Urabe, S. Takeyama, H. Ogura, and H. Yabuki, " $K$ -band receiver front-end IC Integrating micromachined filter and flip-chip assembled active devices," in *IEEE MTT-S Int. Microwave Symp. Dig.*, June 1999, pp. 229–232.

- [9] H. Yabuki, M. Sagawa, M. Matsuo, and M. Makimoto, "Stripline dual-mode ring resonators and their application to microwave devices," *IEEE Trans. Microwave Theory Tech.*, vol. 44, pp. 723–729, May 1996.
- [10] M. Matsuo, H. Yabuki, M. Sagawa, and M. Makimoto, "Analysis of resonant characteristics for a one-wavelength ring resonator coupled with two orthogonal resonant modes," *IEICE Trans. Electron.*, vol. J1-C-1, no. 10, pp. 590–598, Oct. 1998.



**Kazuaki Takahashi** (M'99) was born in Kanagawa, Japan, in 1963. He received the B.E. and M.E. degrees in electrical and computer engineering from Yokohama National University, Yokohama, Japan, in 1986 and 1988, respectively.

In 1988, he joined the Tokyo Research Laboratory, Matsushita Electric Industrial Company Ltd., Kawasaki Japan, where he was engaged in research and development of microwave ICs for mobile communication equipment. In 1996, he joined the Matsushita Research Institute Tokyo Inc., Kawasaki, Japan. His current research interests are millimeter-wave devices and broad-band wireless communication systems.

Mr. Takahashi is a member of the Institute of Electronics, Information and Communication Engineers (IEICE), Japan.



**Ushio Sangawa** was born in Kagawa, Japan, in 1965. He received the B.Sc. degree in physics from the Science University of Tokyo, Tokyo, Japan, in 1989, and the M.Sc. degree in physics from Tohoku University, Sendai, Japan, in 1991.

In 1991, he joined Matsushita Research Institute Tokyo Inc., Kawasaki, Japan. His research interests are in the field of millimeter-wave passive devices and antennas incorporating micromachining technology and photonic concepts.



**Suguru Fujita** was born in Japan, in 1968. He received the B.S. degree in electrical engineering from Waseda University, Tokyo, Japan, in 1990.

In 1991, he joined the Matsushita Electric Industrial Company Ltd., Kawasaki, Japan, where he performed research and development work on microwave components. In 1996, he joined the Matsushita Research Institute Tokyo Inc., Kawasaki, Japan, where he has been engaged in development of microwave equipment for advanced mobile communication systems.

Mr. Fujita is a member of the Institute of Electronics, Information and Communication Engineers (IEICE), Japan.



**Michiaki Matsuo** was born in Japan, in 1967. He received the B.S. and M.S. degrees in electrical engineering from Waseda University, Tokyo, Japan, in 1990 and 1992, respectively.

In 1992, he joined the Matsushita Electric Industrial Company Ltd., Kawasaki, Japan, where he performed research and development on microwave components, particularly resonators and filters. In 1996, he joined the Matsushita Research Institute Tokyo Inc., Kawasaki, Japan, where he has been engaged in development of microwave equipment

for advanced mobile communication systems.

Mr. Matsuo is a member of the Institute of Electronics, Information and Communication Engineers (IEICE), Japan.



**Takeharu Urabe** was born in Japan, in 1969. He received the B.E. and M.E. degrees in mechanical engineering from Kansai University, Osaka, Japan, in 1993 and 1995, respectively.

In 1995, he joined the Matsushita Electric Industrial Company Ltd., Osaka, Japan. In 1997, he joined the Matsushita Research Institute Tokyo Inc., Kawasaki, Japan. In 2000, he joined the Matsushita Electric Industrial Company Ltd., Kawasaki, Japan, where he has been engaged in development of millimeter-wave devices using silicon micromachining

technology.



**Hiroshi Ogura** was born in Tokyo, Japan, on May 3, 1961. He received the B.Eng. degree in mechanical engineering from the University of Electro-Communications, Tokyo, Japan, in 1985.

In 1985, he joined the Production Engineering Laboratory, Matsushita Electrical Industrial Company Ltd., Osaka, Japan, where he performed research and development on semiconductor manufacturing equipment, especially dry-etching systems. In 2000, he joined the Advanced Technology Research Laboratories, Matsushita Electric Industrial

Company Ltd., Kawasaki, Japan, where he is currently engaged in the research and development of millimeter-wave devices for advanced radio systems.

Mr. Ogura is a member of the Institute of Electrical Engineers of Japan.



**Hiroyuki Yabuki** was born on February 28, 1961, in Chiba, Japan. He received the B.S. and Dr.Eng. degrees in electrical engineering from Keio University, Yokohama, Japan, in 1984 and 2000, respectively.

In 1984, he joined the Matsushita Research Institute Tokyo Inc., Kawasaki, Japan, where he performed research and development on UHF radio circuits for mobile communication systems. He is currently concerned with microwave and millimeter-wave ICs and components. He is also engaged in research and development of radio

equipment for advanced mobile communication systems.

Dr. Yabuki is a member of the Institute of Electronics, Information and Communication Engineers (IEICE), Japan.